Additional Acoustic Method for Measuring Formation Permeability in the Presence of Mudcake Achieved (Russian)

Article · January 2012

DOI: 10.2118/160357-RU

CITATIONS
0

READS
45

3 authors, including:

Evgeniy Romenski
Russian Academy of Sciences
141 PUBLICATIONS **1,775** CITATIONS
SEE PROFILE

Vitaly Nikolaevech Dorovsky
Baker Hughes Incorporated
51 PUBLICATIONS **233** CITATIONS
SEE PROFILE

Available online at www.sciencedirect.com
ScienceDirect
Russian Geology and Geophysics 53 (2012) 829–834
RUSSIAN GEOLOGY AND GEOPHYSICS
www.elsevier.com/locate/rgg

Effects of a mudcake on Stoneley waves in a fluid-filled porous formation around a borehole

A.V. Sinev [a,*], E.I. Romensky [a,b], V.N. Dorovsky [a]

[a] *Baker Hugues, Russian Science Center, ul. Kutateladze 4A, Novosibirsk, 630128, Russia*
[b] *Sobolev Institute of Mathematics, Siberian Branch of the Russian Academy of Sciences, pr. Akademika Koptyuga 4, Novosibirsk, 630090, Russia*

Received 13 April 2011; accepted 21 October 2011
Available online xx July 2012

Abstract

A mudcake developed on the borehole wall between a fluid-filled porous formation and the borehole fluid can affect Stoneley wave propagation used to estimate the formation permeability. The mudcake effect on the permeability dependence of radial oscillations of borehole fluid is investigated in a system with a source generating radial acoustic waves in the borehole and geophones (pressure sensors) that record the respective attenuating oscillations of the borehole fluid. The permeability of the porous formation is estimated from theoretical permeability dependence of the attenuation exponent, knowing the time dependence of the exponential attenuation of borehole fluid oscillations.

Keywords: Stoneley waves; permeability; mudcake

Introduction

Propagation of borehole Stoneley waves in fluid-filled porous formations has important implications for reservoir permeability as the latter controls the Stoneley phase velocity and attenuation. The permeability dependence of attenuation length is a zero-order effect, i.e., the Stoneley wave does not attenuate at zero permeability but attenuates in permeable solids. This dependence makes Stoneley wave parameters good proxies to study the structure of porous solids (Xianyun and Hezhu, 2007).

Drilling with the existing technology produces a mudcake on the borehole wall between the borehole fluid and the porous formation while the mudcake rheology (shear response, viscosity, etc.) is most often unknown. Thus a question arises of how the mudcake effect can interfere with the behavior of the formation permeability, the principal object of our interest, derived from measured Stoneley wave parameters. Namely, how the mudcake size and rheology influence the Stoneley attenuation length and group velocity. This is by no means an idle question, and the answer is not obvious at all.

If the mudcake is thin enough, the Stoneley wave, being a surface wave in a porous solid, has an asymptotic "spatial coda" which corresponds to its attenuation and allows using it as a permeability indicator. On the other hand, in the case of a rather thick mudcake, there are two interacting Stoneley waves along its both sides, and non-elastic rheology of the mudcake may cause anomalous dissipation patterns.

A mudcake developed on the borehole wall is expected also to modify the permeability dependence of radial oscillations of borehole fluid, another physical effect essential in measuring formation permeability (Dorovsky et al., 2011), and the measurement procedure has to change correspondingly. In a system operated at the resonance frequency of the borehole's natural radial oscillations and subject to forced oscillations, the velocity difference at the solid/fluid interface is highly sensitive to the permeability of the porous formation around the borehole. Then, the formation permeability can be derived from the interfacial velocity difference measured from the side of the borehole. If there is a mudcake between the borehole and the formation, the interfacial solid/fluid velocity difference still depends on permeability in its vicinity but can no longer be measured directly in the borehole. However, remaining permeability-dependent, the solid/fluid velocity difference in the formation outside the borehole records the effective attenuation of borehole fluid oscillations. This may be the way of measuring formation permeability in the presence of a mudcake. In this respect it appears reasonable to investigate Stoneley wave dissipation in the vicinity of a mudcake.

Liu and Johnson (1997) modeled the effect of a mudcake as an elastic impermeable layer (a membrane) on tube

* Corresponding author.
E-mail address: Sinev@bakerhughes.com (A.V. Sinev)

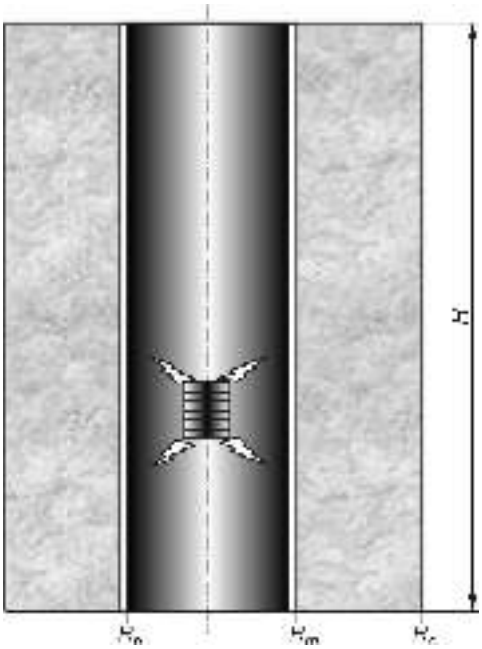

Fig. 1. Model system consisting of a borehole in a porous formation and a mudcake on the borehole wall. See text for explanation.

(Stoneley) wave propagation in porous formations in terms of the Biot theory. As they found out, the mudcake can reduce, but not eliminate, the permeability effects on the tube wave slowness and attenuation. It should be noted, however, that the way of reporting data as frequency dependences of Stoneley wave parameters in (Liu and Johnson, 1997) poses problems to interpretation and to checking against experimental data. Maximov and Merkulov (2002) investigated the effects of a mudcake either as an elastic layer or as a viscous fluid, in a low-frequency approximation. They likewise reported the results as frequency dependences and concluded that the mudcake rheology caused a marked effect on the permeability dependence of Stoneley wave propagation.

Borehole fluid, viscoelastic layer, permeable formation

In this study we model numerically the propagation of waves generated by a source in a finite-size formation sample (Fig. 1), which is a cylinder of the height H and the radius R_c, with a coaxial borehole of the radius R_b at its center. A thin cylindrical layer between the borehole and the cylinder simulates a mudcake. The mudcake/formation interface has the radius R_m. The borehole is filled with fluid, and the same fluid saturates the porous formation sample. The mudcake layer is impermeable for fluid and lines tightly the permeable formation preventing fluid leakage from the latter.

The equations for acoustic waves in the model are: acoustic equations for the borehole fluid; two-velocity linearized equations (Blokhin and Dorovsky, 1995) for the fluid-filled formation (porous solid); Maxwell's linear equations for viscoelastic solids (Godunov and Romenskii, 2003) for the mudcake. The mudcake parameters in the model are borrowed from (Maximov and Merkulov, 2002). The relaxation time of shear stress, being unknown, is allowed to vary.

Thus, the equations are as follows:

(1) for the borehole fluid

$$\frac{\partial \rho_{00} v_z}{\partial t} + \frac{\partial p}{\partial r} = 0, \quad \frac{\partial \rho_{00} v_z}{\partial t} + \frac{\partial p}{\partial z} = 0,$$

$$\frac{\partial p}{\partial t} + \frac{\partial}{\partial r}(\rho_{00} c^2 v_r) + \frac{\partial}{\partial r}(\rho_{00} c^2 v_z) = -\frac{\rho_{00} c^2 v_r}{r},$$

where v_r, v_z are the velocities along the axes r, z; p is the pressure; ρ_{00}, c are the density and sound velocity, respectively;

(2) for the viscoelastic mudcake

$$\rho_e \frac{\partial w_r}{\partial t} - \frac{\partial \sigma_{rr}}{\partial r} - \frac{\partial \sigma_{rz}}{\partial z} = \frac{2\mu_e}{r}(\varepsilon_{rr} - \varepsilon_{\varphi\varphi}),$$

$$\rho_e \frac{\partial w_z}{\partial t} - \frac{\partial \sigma_{rz}}{\partial r} - \frac{\partial \sigma_{zz}}{\partial z} = \frac{2\mu_e}{r}\varepsilon_{rz},$$

$$\frac{\partial \varepsilon_{rr}}{\partial t} - \frac{\partial w_r}{\partial r} = -\frac{1}{\tau}\left(\varepsilon_{rr} - \frac{\varepsilon_{rr} + \varepsilon_{\varphi\varphi} + \varepsilon_{zz}}{3}\right),$$

$$\frac{\partial \varepsilon_{\varphi\varphi}}{\partial t} = \frac{w_r}{r} - \frac{1}{\tau}\left(\varepsilon_{\varphi\varphi} - \frac{\varepsilon_{rr} + \varepsilon_{\varphi\varphi} + \varepsilon_{zz}}{3}\right),$$

$$\frac{\partial \varepsilon_{zz}}{\partial t} - \frac{\partial w_z}{\partial z} = -\frac{1}{\tau}\left(\varepsilon_{zz} - \frac{\varepsilon_{rr} + \varepsilon_{\varphi\varphi} + \varepsilon_{zz}}{3}\right),$$

$$\frac{\partial \varepsilon_{rz}}{\partial t} - \frac{1}{2}\frac{\partial w_z}{\partial r} - \frac{1}{2}\frac{\partial w_r}{\partial z} = -\frac{1}{\tau}\varepsilon_{rz}.$$

where w_r, w_z are the velocities along the axes r, z; σ_{rr}, σ_{rz}, σ_{zz} are the elastic stresses related to the elastic strains ε_{rr}, ε_{rz}, ε_{zz}, $\varepsilon_{\varphi\varphi}$ as (Hooke's law)

$$\sigma_{rr} = (\lambda_e + 2\mu_e)\varepsilon_{rr} + \lambda_e \varepsilon_{\varphi\varphi} + \lambda_e \varepsilon_{zz}, \quad \sigma_{rz} = 2\mu_e \varepsilon_{rz},$$

$$\sigma_{zzr} = \lambda_e \varepsilon_{rr} + \lambda_e \varepsilon_{\varphi\varphi} + (\lambda_e + 2\mu_e)\varepsilon_{zz}$$

where λ_e, μ_e are the Lamé constants, ρ_e is the density, and is the relaxation time of shear stress;

(3) for the saturated porous solid

$$\frac{\partial}{\partial t}(\rho_s u_r + \rho_l v_r) + \frac{\partial}{\partial r}(p + h_{rr}) + \frac{\partial}{\partial z} h_{rz} = -(h_{rr} - h_{\varphi\varphi})/r,$$

$$\frac{\partial}{\partial t}(\rho_s u_z + \rho_l v_z) + \frac{\partial}{\partial r} h_{rz} + \frac{\partial}{\partial z}(p + h_{zz}) = -h_{rz}/r,$$

$$\frac{\partial}{\partial t}\rho_s (u_r - v_r) + \frac{\partial}{\partial r} h_{rr} + \frac{\partial}{\partial z} h_{rz} =$$

$$-(h_{rr} - h_{\varphi\varphi})/r - \rho_0 \rho_l \chi (u_r - v_r),$$

$$\frac{\partial}{\partial t}\rho_s (u_z + v_z) + \frac{\partial}{\partial r} h_{rz} + \frac{\partial}{\partial z} h_{zz} = h_{rz}/r - \rho_0 \rho_l \chi (u_z - v_z),$$

$$\frac{\partial}{\partial t}\rho/\rho_0 + \frac{\partial}{\partial r}(\rho_s u_r + \rho_l v_r)/\rho_0 + \frac{\partial}{\partial z}(\rho_s u_z + \rho_l v_z)/\rho_0 =$$

$$-(\rho_s u_r + \rho_l \nu_r)/\rho_0/r,$$

$$\frac{\partial \varepsilon_{rr}}{\partial t} - \frac{\partial u_r}{\partial r} = 0, \quad \frac{\partial \varepsilon_{\varphi\varphi}}{\partial t} = \frac{U_r}{r},$$

$$\frac{\partial \varepsilon_{zz}}{\partial t} - \frac{\partial u_z}{\partial z} = 0, \quad \frac{\partial \varepsilon_{rz}}{\partial t} - \frac{1}{2}\frac{\partial u_z}{\partial r} - \frac{1}{2}\frac{\partial u_r}{\partial z} = 0,$$

where ρ is the deviation of the formation bulk density from the original equilibrium value ρ_0; $\rho_s = (1-\Phi)\rho_s^f$, and $\rho_l = \Phi\rho_l^f$ are the partial densities of the elastic solid and the saturating fluid, respectively; ρ_s^f, ρ_l^f are the mass densities of the solid and the fluid, respectively; $\rho_0 = \rho_s + \rho_l$ is the formation bulk density; u_r, u_z are the velocities of the solid along the axes r, z; ν_r, ν_z are the velocities of the fluid along the axes r, z; ε_{rr}, ε_{zz}, ε_{rz}, $\varepsilon_{\varphi\varphi}$ is the strain tensor of the elastic solid; p is the pressure; h_{rr}, h_{zz}, h_{rz}, $h_{\varphi\varphi}$ are the stress tensors related with the density and with the strain tensor as

$$p = K(\varepsilon_{rr} + \varepsilon_{zz} + \varepsilon_{\varphi\varphi}) + (K + \rho_0^2\alpha_3)\frac{\rho}{\rho_0},$$

$$h_{rr} = -(\lambda + 2\mu)\varepsilon_{rr} - \lambda\varepsilon_{\varphi\varphi} - \lambda\varepsilon_{zz} - K\frac{\rho}{\rho_0},$$

$$h_{\varphi\varphi} = -\lambda\varepsilon_{rr} - (\lambda + 2\mu)\varepsilon_{\varphi\varphi} - \lambda\varepsilon_{zz} - K\frac{\rho}{\rho_0},$$

$$h_{zz} = -\lambda\varepsilon_{rr} - \lambda\varepsilon_{\varphi\varphi} - (\lambda + 2\mu)\varepsilon_{zz} - K\frac{\rho}{\rho_0},$$

$$h_{rz} = -2\mu\varepsilon_{rz},$$

where K, λ, μ, α_3 are the elastic constants; χ is the interfacial friction coefficient.

The conditions at the interfaces between the fluid, the elastic mudcake, and the saturated porous solid are as follows.

fluid—mudcake:

$\nu_r = w_r$: continuity of radial velocity,

$p = -\sigma_{rr}$: continuity of radial stress,

σ_{rz}: absence of shear stress relative to the interface;

mudcake—saturated porous solid:

$p_e w_r = \rho_l \nu_r + (\rho_e - \rho_l) u_r$: balance of mass flow across the interface (the interface is assumed to move at the same velocity as the elastic solid),

$-\sigma_{rr} = \frac{\rho_l}{\rho} p + \frac{\rho_s}{\rho} p + h_{rr}$: continuity of radial stress,

$-(1-\Phi)\sigma_{rr} = \frac{\rho_s}{\rho} p + h_{rr}$: continuity of partial stresses of the solid and the mudcake,

$h_{rz} = -\sigma_{rz}$: continuity of shear stress relative to the interface,

$w_z = u_z$: continuity of velocity along the interface (no slip).

Free boundary conditions are

At $z = H$:

fluid

$p = 0$: absence of exterior pressure;

mudcake

$\sigma_{zz} = 0$, $\sigma_{rz} = 0$: absence of normal and shear stresses;

saturated porous solid

$p/\rho_0 + h_{zz} = 0$, $h_{rz} = 0$, $u_z - \nu_z = 0$: absence of normal and shear stresses; absence of leakage through the solid's surface.

At $r = R_c$:

saturated porous solid

$p/\rho_0 + h_{rr} = 0$, $h_{rz} = 0$, $u_r - \nu_r = 0$: absence of normal and shear stresses; absence of leakage through the surface $r = R_c$ of the porous solid.

The lower boundary of the modeling domain $z = 0$ is a symmetry plane, where the following boundary conditions are fulfilled:

fluid

$\nu_z = 0$,

mudcake

$w_z = 0$, $\sigma_{rz} = 0$,

saturated porous solid

u_z, $h_{rz} = 0$, $\nu_z = 0$.

The source that generates borehole fluid oscillations is a cylinder coaxial with the borehole, with its radius smaller than the borehole radius R_b, and the height from 0 to H. The bottom of the cylinder may lie at a randomly set point. Acoustic waves are generated by harmonic pressure $p(t)$ at the source boundary. After the source has been off, its boundary is assumed to be a stiff wall with zero normal velocity ($\nu_n = 0$).

The numerical solutions reported below are for two 2D problems of wave propagation from a source on the borehole axis. The modeling is using a 2D code (Dorovsky et al., 2011) based on Godunov-type high-order accurate finite-difference scheme, with the WENO (Weighted Essentially Non-Oscillatory) and Runge-Kutta algorithms for space and time, respectively (Toro, 2009).

Stoneley attenuation

The Stoneley wave is a key component of the borehole wavefield in a porous formation. It attenuates in porous solids because of energy dissipation and its attenuation patterns thus have implications for the formation properties. In this section the Stoneley attenuation is modeled in 2D in the presence of a mudcake developed on the borehole wall. The problem is symmetrical about the plane $z = 0$. A cylindrical finite-size source located on the borehole axis occupies the domain $[0, R_s] \times [0, h]$. Pressure is recorded by geophones placed near the borehole wall and spaced at 0.03 m. The first geophone is at the distance 0.1 m from the plane $z = 0$. The modeling domain parameters are as follows: the height 0.5 m and the radius 0.2 m; the borehole radius 0.04 m; the source radius 0.01 m; height 0.02 m. The mudcake thicknesses are 6.0×10^{-4} m, 1×10^{-3} m, 2×10^{-3} m, and 3×10^{-3} m. In the Maxwell viscoelastic model, the shear stress relaxation times are allowed to vary. The formation permeability is from 1 mD to 10D. The parameters for the three types of media in the problem are: fluid of the density 10^3 and the acoustic

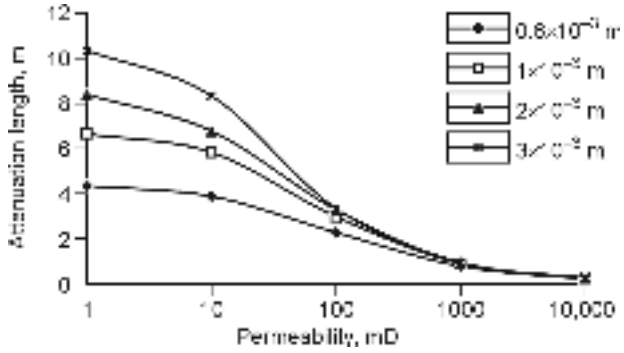

Fig. 2. Permeability dependence of Stoneley attenuation for different mudcake thicknesses.

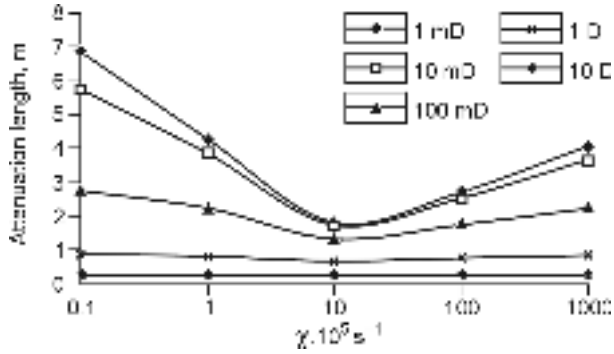

Fig. 3. $\chi = 1/\tau$ dependence of attenuation length for different permeabilities.

velocity 1.5×10^3 m/s; mudcake with the density 1.1×10^3 kg/m^3, the compressional velocity 1.5×10^3 m/s, and shear velocity 0.32×10^3 m/s; fluid-filled porous solid with the densities of the solid and the fluid 2.5×10^3 kg/m^3 and 1.0 g/cm^3, respectively, and with the fast and slow P velocities 3.5×10^3 m/s and 1.2×10^3 m/s, respectively; the S velocity is 2.4×10^3 m/s, and the porosity is 0.2. The source of acoustic waves is defined by time-dependent pressure on the surface $p = p(t) = p_0 \sin(10^5 \pi t)$, $t < 10^{-5}$ s. After the pressure source has been off, its boundary becomes a stiff wall with zero normal velocity $v_r = 0$. The results are presented as time dependences of pressure for each geophone, wherefrom the Stoneley wave is picked.

In Figure 2 Stoneley attenuation length is plotted against permeability for different mudcake thicknesses. It is generally greater at greater mudcake thicknesses. As permeability increases, the attenuation length decreases, for all mudcake thicknesses, and tends to zero in the high permeability limit, the wave attenuation being spatially asymptotic. As a consequence, all curves coalesce in a single line in the high-permeability region. In other words, the attenuation length is almost independent of mudcake thickness at high permeabilities. The obtained empirical formula relating attenuation length, mudcake thickness, and permeability is $k \sim \exp(-1.4 \cdot L/\sqrt{h})$, where k is the permeability, h is the mudcake thickness (in meters), and L is the attenuation length (in meters). Note that the attenuation length becomes more sensitive to permeability as the mudcake thickness increases.

Figure 3 illustrates modeling for the case of a mudcake being a Maxwell viscoelastic solid. The attenuation length is plotted as a function of $\chi = 1/\tau$, which is the inverse relaxation time (measured in 10^5 1/s) for different permeabilities of 1 mD, 10 mD, 100 mD, 1 D, and 10 D. The attenuation length only weakly depends on shear stress relaxation at high permeabilities and shows an anomalous decrease at $\tau \sim 10^{-6}$ s. The mudcake thickness is assumed to be $h = 2.0 \times 10^3$ m, and the Stoneley velocity is of the order 1.3×10^3 m/s. The characteristic traveltime of the acoustic wave across the mudcake is ~10^{-6} s. Thus, at a characteristic shear stress relaxation time commensurate with the acoustic wave traveltime across the mudcake, the pattern looks like that at high permeabilities. The latter fact can lead to misinterpretation of permeability inferred from Stoneley dissipation. As Fig. 3 shows, neglect of the mudcake rheology causes errors to permeability estimates, especially at large relaxation times and low permeabilities.

The permeability-dependent Stoneley attenuation length for different relaxation times $\chi = 1/\tau = 0.1$; 1.0; 10.0; 100.0; 1000.0 ($\times 10^5$ 1/s) (Fig. 4) shows no sensitivity to the mudcake rheology at high permeabilities.

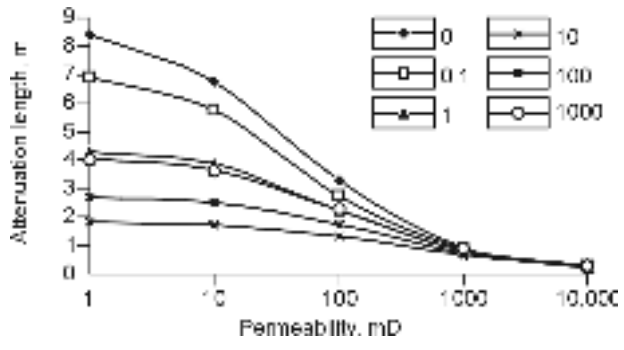

Fig. 4. Permeability dependence of attenuation length for different relaxation times.

Stoneley velocity

The Stoneley velocity is easy to measure with a system of geophones along the borehole wall. The permeability-dependent Stoneley velocity for the case of an elastic mudcake of the thickness 0.6×10^{-3} m, 1.0×10^{-3} m, 2.0×10^{-3} m, 3.0×10^{-3} m (Fig. 5), with the model parameters as above, is in the range 1300 m/s. Its dependence on both the mudcake thickness and the formation permeability, is quite weak. With the shear stress relaxation included into the calculations, the Stoneley velocity estimates change negligibly.

The curves of Fig. 6 are permeability dependences of the Stoneley velocity for different relaxation times $\chi = 1/\tau$,

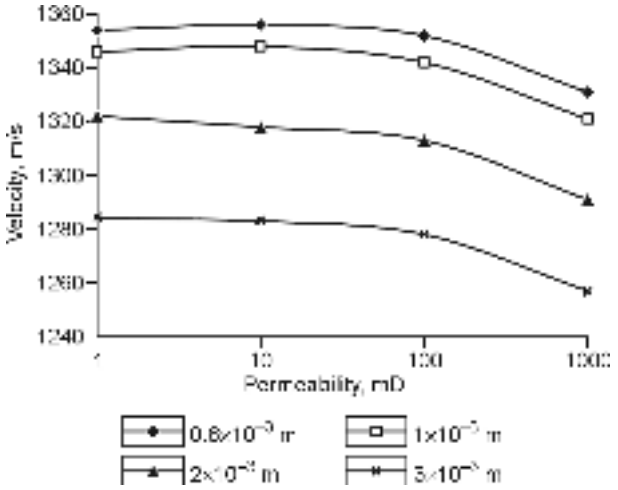

Fig. 5. Permeability dependence of Stoneley velocity for a mudcake being an elastic layer.

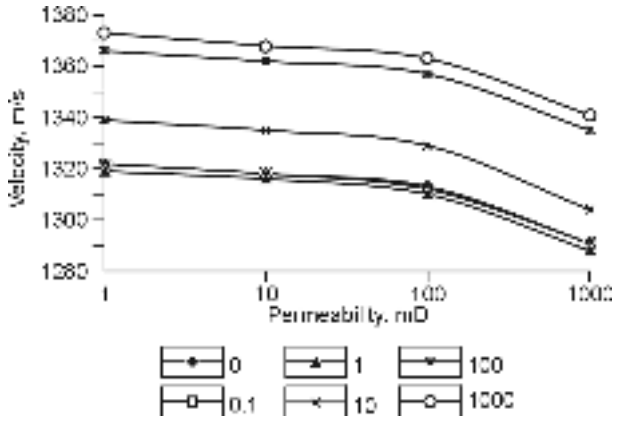

Fig. 6. Permeability dependence of Stoneley velocity for different relaxation times.

namely, for $\chi = 0$; 0.1; 1.0; 10.0; 100.0; 1000.0 in 10^5 1/s. At $\chi = 0$, the mudcake is elastic while at $\chi = 10^8$ it corresponds to a fluid with the dynamic viscosity $\eta = 11.264 \times 10^{-5}$ kg/(m·s). At large relaxation times (an almost elastic mudcake), the Stoneley velocity decreases slightly as the relaxation time τ decreases. Then, with further τ decrease, the velocity begins to grow approaching its limit in the case of an ideal fluid in the borehole and in the pore space.

This effect is prominent in the $\chi = 1/\tau$ dependence of Stoneley velocity (Fig. 7) plotted for the permeabilities 1 mD, 10 mD, 100 mD, 1 D. The reason is that two Stoneley waves traveling along the fluid/mudcake and mudcake/porous solid interfaces, respectively, interact and the latter wave actually travels along the fluid/solid interface as the relaxation time decreases.

Radial oscillations

In (Dorovsky et al., 2011) resonance radial oscillations of borehole fluid were employed for estimating the permeability of porous reservoirs, proceeding from the fact that the interfacial velocity difference between the porous solid and the fluid is highly sensitive to the permeability of the formation outside the borehole at the resonance frequency. However, the method requires special instruments to measure the velocity difference. Furthermore, it does not work in the presence of a mudcake on the borehole wall because direct borehole measurements of the velocity difference become impossible while the permeability dependence of this velocity still holds at the mudcake/formation interface. Below we suggest an alternative technique of estimating formation permeability around the borehole, both in the presence and in the absence of a mudcake.

The amplitude of pressure oscillations in the borehole fluid can be expected to attenuate because the solid/fluid interfacial velocity difference still depends on formation permeability outside the mudcake. However, attenuation likewise includes a component associated with constant generation of waves moving from the oscillating fluid to the periphery. The permeability dependence of borehole pressure attenuation has to be distinguished in the explicit form.

Figure 8 illustrates the attenuation of borehole fluid pressure produced by a primary acoustic source of radial oscillations for the case of a 1×10^{-3} m thick mudcake and the formation permeability 1 mD. Figures 9 and 10 show exponential time dependence of borehole pressure for four perme-

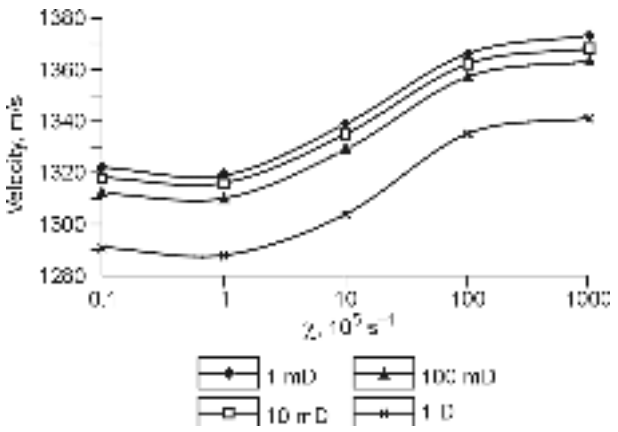

Fig. 7. $\chi = 1/\tau$ dependence of Stoneley velocity for different permeabilities.

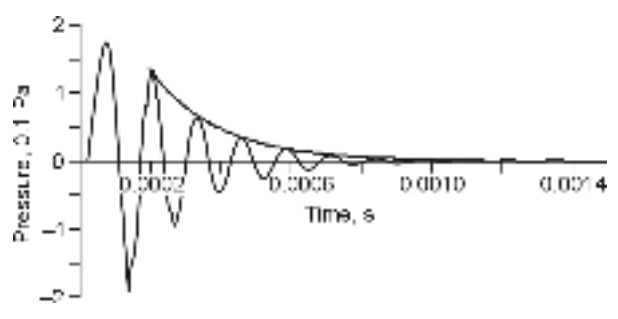

Fig. 8. Time-dependent pressure for mudcake thickness 1 mm and permeability 1 mD, and approximation of extremes by $e^{-5142.8t}$.

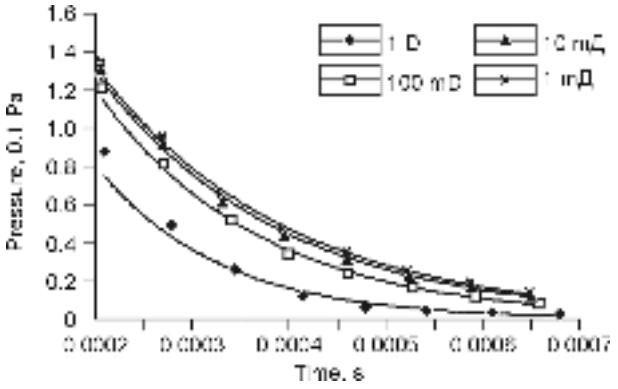

Fig. 9. Time-dependent extreme magnitudes of acoustic fluid pressure at fluid/mudcake interface, for mudcake thickness 1.0×10^{-3} m, at different permeabilities, and approximation of the dependence by $e^{-\alpha t}$.

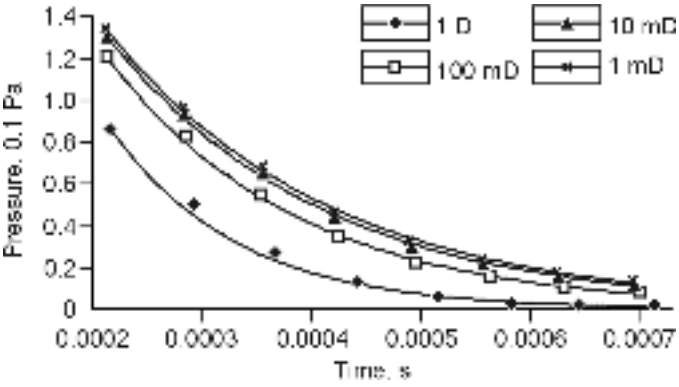

Fig. 10. Time-dependent extreme magnitudes of acoustic fluid pressure at fluid/mudcake interface, for mudcake thickness 3.0×10^{-3} m, at different permeabilities at two mudcake thicknesses. The pressure magnitudes for the permeabilities $k = 1$ mD, 10 mD, 100 mD, 1 D and the mudcake thickness 1×10^{-3} m are approximated by the exponents $e^{-\alpha t}$ (Fig. 9). In Figure 11, the permeability-dependent exponents α are compared for the mudcake thicknesses 1×10^{-3} m and 3×10^{-3} m.

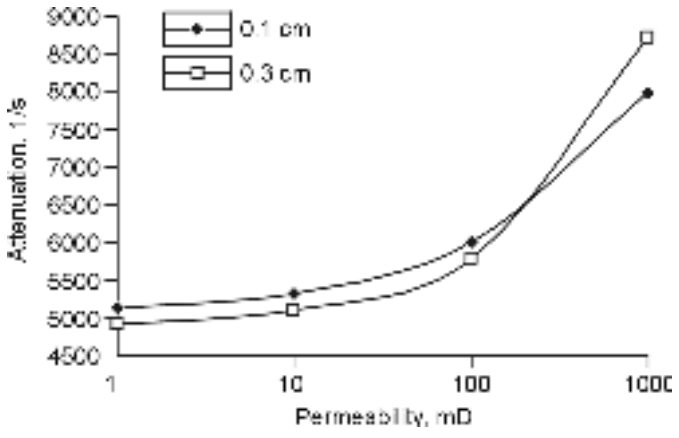

Fig. 11. Permeability dependence of attenuation (exponent of α that approximates extreme magnitudes of acoustic fluid pressure) at borehole/formation interface, for mudcake thicknesses 1.0×10^{-3} m and 3.0×10^{-3} m.

Note that although the pressure attenuation becomes less sensitive to formation permeability as the latter decreases to less than 10 mD, high precision of pressure measurements still allows resolving the permeability. Thus, the permeability of a formation outside the borehole can be inferred unambiguously, both in the absence and in the presence of a mudcake, knowing the exponent of time-dependent pressure attenuation, as well as the formation density, porosity, and three acoustic velocities.

The wavefields are modeled in this case using a 1D version of the equation system given above. The use of a 1D version of the method from (Dorovsky et al., 2011) is possible for a cylindrical source along the whole borehole axis. The geophone (pressure sensor) is placed near the borehole wall. The modeling domain is unbounded along the radius, following the new perfectly matched layer (PML) model of Appelö and Kreiss (2006); the borehole radius is 0.04 m and the source radius is 0.01 m. The parameters of the three media are:

- *fluid*: density 10^3 kg/m^3, acoustic velocity 1.5×10^3 m/s;
- *mudcake*: density 1.1×10^3 kg/m*3*, *P* velocity 1.5×10^3 m/s, *S* velocity 0.32×10^3 m/s;
- *saturated porous solid*: density of solid 2.5×10^3 kg/m^3, density of fluid 10^3 kg/m^3, fast *P* velocity 3.5×10^3 m/s, slow *P* velocity 1.2×10^3 m/s, *S* velocity 2.4×10^3 m/s, porosity 0.2.

In the beginning of the process, the source of acoustic waves is defined by time-dependent pressure at the source-fluid interface: $p = p(t) = p_0 \sin(10^4 \pi t)$. After the pressure source has been off, its boundary becomes a stiff wall where $v_r = 0$.

References

Appelö, D., Kreiss, G., 2006. A new absorbing layer for elastic waves. J. Comput. Phys. 215 (2), 642–660.

Blokhin, A.M., Dorovsky, V.N., 1995. Mathematical Modeling in the Theory of Multivelocity Continuum. New York: Nova Science Publishers Inc.

Dorovsky, V.N., Romensky, E.I., Fedorov, A.Yu., Perepechko, Yu.V., 2011. A resonance method for measuring permeability. Russian Geology and Geophysics (Geologiya i Geofizika) 52 (7), 745–752 (950–961).

Godunov, S.K., Romensky, E.I., 2003. Elements of continuum mechanics and conservation laws. Kluwer Academic/Plenum Publishers, NY,

Liu, H.-L., Johnson, D.L., 1997. Effects of an elastic membrane on tube waves in permeable formations. J. Acoust. Soc. Am. 101 (1), 3322–3329.

Maximov, G.A., Merkulov, M.E., 2002. Effect of a mudcake on the propagation of Stoneley waves in a borehole. Acoustical Physics 48 (2), 187–200.

Toro, E.F., 2009. Riemann Solvers and Numerical Methods for Fluid Dynamics. 3rd edition, Springer.

Xianyun, W., Hezhu, Y., 2007. Method for determining reservoir permeability from borehole Stoneley-wave attenuation using Biot's poroelastic theory. Patent No. WO/2007/001746.

Editorial responsibility: M.I. Epov